Joint Centre for Mesoscale Meteorology, Reading, UK

Deriving cloud overlap statistics from radar

A. J. Illingworth
R. J. Hogan

Internal Report No. 125
NWP Scientific Paper No. 339

January 2001

Met Office Joint Centre for Mesoscale Meteorology Department of Meteorology
University of Reading PO Box 243 Reading RG6 6BB United Kingdom
Tel: +44 (0)118 931 8425 Fax: +44 (0)118 931 8791
www.metoffice.com

Designed and produced by the Met Office © Crown copyright 2001 01/0240 The Met Office logo is a registered trademark.

Deriving cloud overlap statistics from radar

ROBIN J. HOGAN* AND ANTHONY J. ILLINGWORTH

Department of Meteorology, University of Reading, United Kingdom

ABSTRACT

The predictions of General Circulation Models (GCMs) are sensitive to the assumed cloud overlap within a vertical column of model gridboxes, but until now no reliable observations of the degree of cloud overlap have been available. In this note we derive the overlap characteristics of clouds from 71 days of high vertical resolution 94-GHz cloud radar data in the UK. It is found that, contrary to the assumption made in most models, vertically continuous clouds tend not to be maximally overlapped. Rather, the overlap of clouds at two levels tends to fall rapidly as their vertical separation is increased, and for levels more than 4 km apart, overlap is essentially random. A simple inverse-exponential expression for the degree of overlap as a function of level separation is proposed that could, once results become available from a variety of other locations and seasons, be implemented in current GCMs with relatively little difficulty.

1. Introduction

The distribution of clouds in the atmosphere represents one of the major uncertainties in our understanding of the present climate (IPCC 1995), and limits our confidence in future climate prediction. General Circulation Models (GCMs) currently carry a value for cloud fraction in each model gridbox but it has been found that different assumptions on the way clouds overlap in a vertical column of gridboxes can have a strong effect on the model radiation budget (Morcrette and Fouquart 1986; Charnock et al. 1994; Liang and Wang 1997; Stubenrauch et al. 1997). This in turn affects circulation patterns (Liou and Zheng 1984; Slingo and Slingo 1988; Randall et al. 1989). The three different cloud overlap assumptions that have commonly been made in GCMs are shown schematically in Fig. 1. Integrations of the European Centre for Medium-Range Weather Forecasts (ECMWF) model by Morcrette and Jakob (2000) highlighted the important differences between them: simulated global-mean cloud cover was 71.4% when random overlap was assumed but only 60.9% in the case of maximum overlap, and over parts of the ITCZ the resulting differences in mean outgoing longwave radiation were in excess of 40 W m^{-2}. While the importance of cloud overlap for radiation has long been recognised, it is only recently that its role in determining the efficiency of precipitation formation has also been studied (Jakob and Klein 1999).

Nearly all GCMs now employ the so-called 'maximum-random' overlap assumption, whereby vertically continuous clouds are assumed to be maximally overlapped while clouds at different heights that are separated by an entirely cloud-free model level are randomly overlapped (Geleyn and Hollingsworth 1979). The passive observational data used to support this approach has so far been very limited in vertical resolution (Tian and Curry 1989). Barker et al. (1999) carried out Monte Carlo simulations of solar fluxes on convective clouds generated with a cloud-resolving model, and found that the overlap of the model clouds differed from the generally-assumed maximum-random overlap, resulting in shortwave flux differences of up to 100 W m^{-2}. They looked forward to a time when overlap could be validated from ground-based and spaceborne radars. In this note we report new results on cloud overlap derived using high vertical resolution millimetre-wave radar. The potential of such instruments for the validation of model cloud fields was demonstrated by Mace et al. (1998) and Hogan et al. (2001).

2. Method

We use the near-continuous observations taken between 6 November 1998 and 24 January 1999 by the ESTEC 94-GHz 'Galileo' radar at Chilbolton, England. This dataset was used by Hogan et al. (2001) to derive cloud fraction for comparison with the values held in the ECMWF model. The radar was vertically-pointing and recorded radar reflectivity factor (Z) as a 10-s average with a vertical resolution of 60 m. A 6.9 dB increase in sensitivity was achieved by averaging over 2 mins and 120 m, resulting in minimum-detectable Z of around -52.5 dBZ at 1 km and -32.5 dBZ at 10 km. The clouds most likely to be undetected by radar are high thin cirrus, but it was shown by Brown et al. (1995) that virtually all 'radiatively-significant' cirrus (essentially that which decreases outgoing longwave radiation by at least 10 W m^{-2}) should be detected by a radar with a minimum-detectable Z of -30 dBZ. A reduction in the sensitivity of the instrument by 5 dB is found to have a negligible effect on the final results, so there is no reason to suppose that very tenuous clouds should have significantly different overlap characteristics from detectable clouds. Nonetheless, we restrict our analysis to data recorded below 10.5 km. Data below 750 m are not used because here the radar sensitivity is somewhat compromised by leakage of the transmit pulse into the receiver. It should be noted that the common problem of data contamination by insects is entirely absent at the latitude of Chilbolton during

*Corresponding author address: Department of Meteorology, Earley Gate, Whiteknights, Reading, Berkshire, RG6 6BB, UK (e-mail: R.J.Hogan@reading.ac.uk).

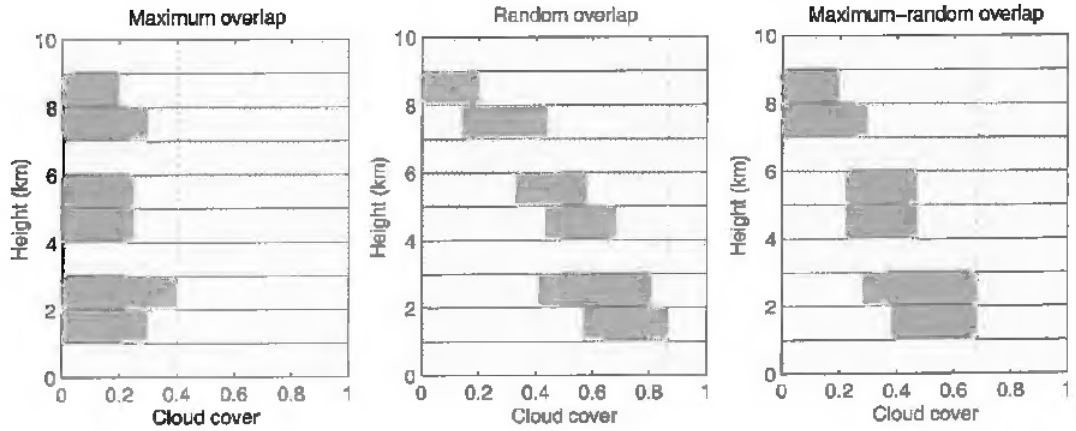

FIG. 1: A schematic illustrating the three overlap assumptions that are commonly made in GCMs. The dotted vertical lines denote total cloud cover. For clarity we have adopted the convention used by Morcrette and Jakob (2000) and drawn only a single cloud at each level. While the total cloud cover from the top of the atmosphere down to any particular level is correct, the use of a single cloud at each level in the diagram is a simplification for the overlap of any two individual layers in the cases of random and maximum-random overlap.

winter.

To compute actual overlap, daily time-height sections of Z were divided into equally-sized boxes, and within each box a simple 'cloud cover mask' was generated consisting of 'bits' stating whether or not cloud was present at any height within the box in each 2-minute period. To mimic the range of vertical and horizontal resolutions of current GCMs, box sizes of 360 m, 720 m, 1080 m and 1440 m in the vertical and 20 mins, 1 hour and 3 hours in time were used. Taking the mean tropospheric horizontal wind speed to be 20 m s^{-1} (estimated from ECMWF model data over Chilbolton during the experimental period), these temporal resolutions translate to horizontal distances of 24 km, 72 km and 216 km respectively, spanning the range of horizontal resolutions used by operation mesoscale models to climate models. Cloud cover (c) was then defined as the fraction of bits in each box that were cloudy. An example of the generation of the cloud cover mask from a 12-hour time-height section of Z is shown in Fig. 2. It might initially appear that a vertical column of gridboxes with 100% cloud cover at every level is indicative of maximum overlap, but in fact nothing can be inferred about overlap when one or more of the levels under consideration is completely cloudy, since all overlap assumptions must predict the same total cloud cover: 100%. From the vertically continuous cloud enclosed by the box between 18 and 19 UTC, it can be seen immediately that as levels further and further apart are considered, maximum overlap becomes an increasingly poor assumption.

In order to quantify this effect, levels were analysed in pairs, with every possible combination of levels being considered, and no 'double-counting'. For each pair, four possible values for the combined cloud cover (C) of the two levels were calculated. The first was the combined cloud cover obtained assuming random overlap, using the standard definition

$$C_{\text{rand}} = c_{\text{a}} + c_{\text{b}} - c_{\text{a}}c_{\text{b}} \tag{1}$$

(where c_{a} and c_{b} are the cloud covers of the lower and upper levels respectively), the second was the value obtained assuming maximum overlap, defined as

$$C_{\text{max}} = \max(c_{\text{a}}, c_{\text{b}}), \tag{2}$$

the third was the value obtained assuming minimum overlap, defined as

$$C_{\text{min}} = \min(1, c_{\text{a}} + c_{\text{b}}), \tag{3}$$

and the fourth was the combined cloud cover that was actually observed, C_{true}. Note that the subscript 'max' corresponds to the maximum *overlap* and not the maximum possible C; in fact C_{max} is the *minimum* possible value of C (see Fig. 1). Pairs in which either of the levels had a cloud cover of zero or unity were rejected, as in these cases all values of C are equal. Hence after averaging over a sufficiently large number of events, the position of the observed $\bar{C}_{\text{true}}$ between $\bar{C}_{\text{max}}$ and $\bar{C}_{\text{rand}}$ (as a function of level separation) will tell us precisely how a radiation scheme ought to weight cloud overlap between the two extremes of maximum and random.

A problem to consider when deriving overlap at 94 GHz is attenuation by liquid water; when heavy rain is present at low levels the radar beam can be completely obscured, resulting in vertical swaths of apparently cloud-free air directly above the rain. This has the effect of increasing the apparent overlap since the erroneously cloud-free regions are stacked on top of each other. We therefore use measurements taken by a drop-counting rain gauge at Chilbolton to reject from the analysis all events for which the rain rate exceeded 0.5 mm hr^{-1} at any time during the sample period. The effect on the derived overlap characteristics was small because less than 10% of the data were removed in this way. The effect of drizzle falling beneath liquid water clouds was investigated by restricting the analysis to regions where the temperature was below 0°C:

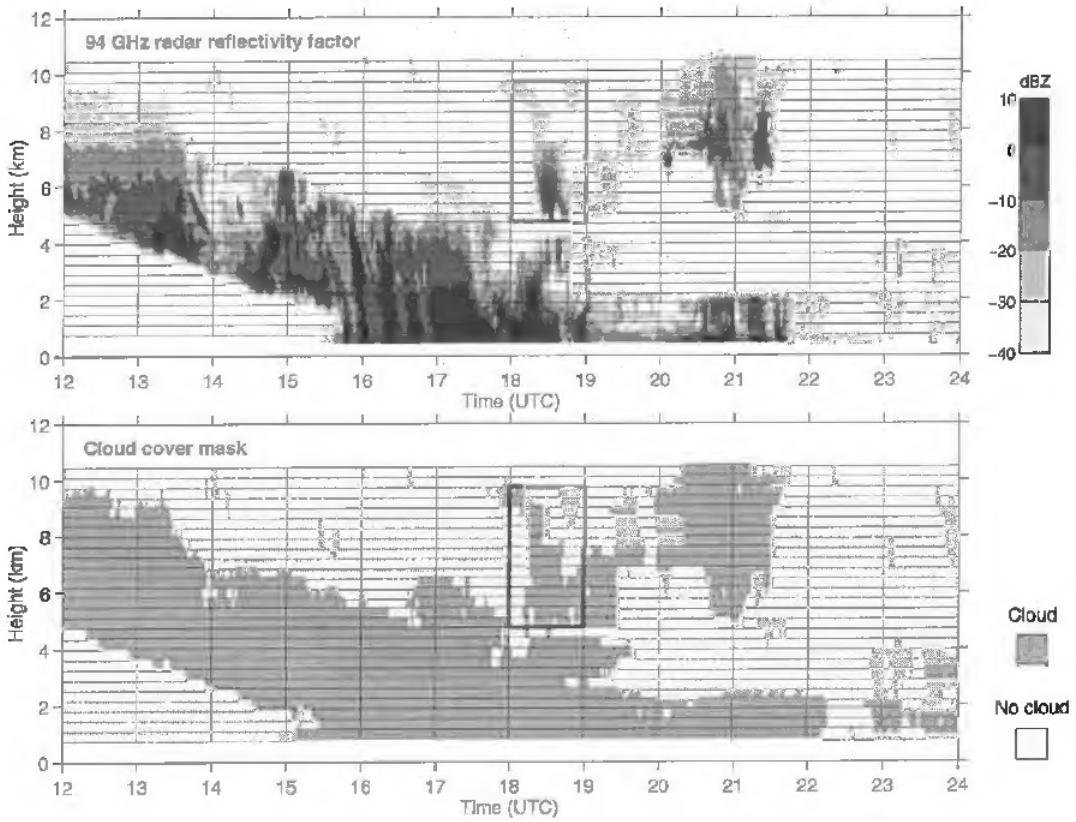

FIG. 2: An example of cloud radar data used to derive the cloud cover mask, from 11 December 1998. Intermittent light drizzle was measured at the ground between 17 and 19 UTC. The resolution of the grid is 360 m and 1 hour.

the change in the overlap statistics was negligible. Another possibility is that large but radiatively-unimportant snow crystals falling beneath ice clouds could be detected by the radar and bias the results. Analysis of simultaneous radar and lidar returns from ice clouds at all heights by Hogan and Illingworth (1999) revealed that this is a rare occurrence; in 94% of their data the radar and lidar cloud base agreed to within 360 m (the highest vertical resolution considered in the present study).

3. Results

The results for boxes measuring 360 m by 1 hour are shown in Fig. 3. Pairs of levels have been grouped together according to their vertical separation, but separated according to whether they are vertically continuous (i.e. the cloud cover in every interstitial level is greater than zero) or non-continuous. We see that in the case of vertically continuous cloud, as the level separation is increased from 360 m to 4 km, $\bar{C}_{\text{true}}$ moves from a value close to that calculated assuming maximum overlap, to essentially the random overlap value. This contrasts with most current GCMs which apply maximum overlap to all vertically continuous levels. In the case of vertically non-continuous cloud on the other hand, there appears to be no significant deviation of $\bar{C}_{\text{true}}$ from that predicted assuming random overlap, in agreement with the schemes used in most GCMs. Of course in individual cases C_{true} takes values anywhere between the extremes of C_{max} and C_{min}.

A simpler and more useful way of presenting these findings is in terms of an 'overlap parameter' α that expresses $\bar{C}_{\text{true}}$ in terms of $\bar{C}_{\text{max}}$ and $\bar{C}_{\text{rand}}$:

$$\bar{C}_{\text{true}} = \alpha \bar{C}_{\text{max}} + (1-\alpha)\bar{C}_{\text{rand}}. \tag{4}$$

Hence $\alpha = 0$ corresponds to random overlap and $\alpha = 1$ to maximum overlap. Figure 4 depicts α as a function of level separation, again for 360 m and 1 hour resolution. The observed values of α would seem to be best fitted by an inverse-exponential of the form

$$\alpha = \exp\left(-\frac{\Delta z}{\Delta z_0}\right), \tag{5}$$

where Δz is the level separation and Δz_0 is an e-folding or 'decorrelation' distance. The value of Δz_0 has been estimated for each of the three temporal resolutions and four vertical resolutions by performing a least-squares fit to the observations, but weighting each observation by the number of events from which the average was calculated. The results are shown in Table 1. Hence if cloud overlap were to be parameterised in models using Eq. 5 then the value of Δz_0 could be chosen to match the model resolution. The weighting is necessary because cloud frequency obviously decreases with increasing physical thickness, and

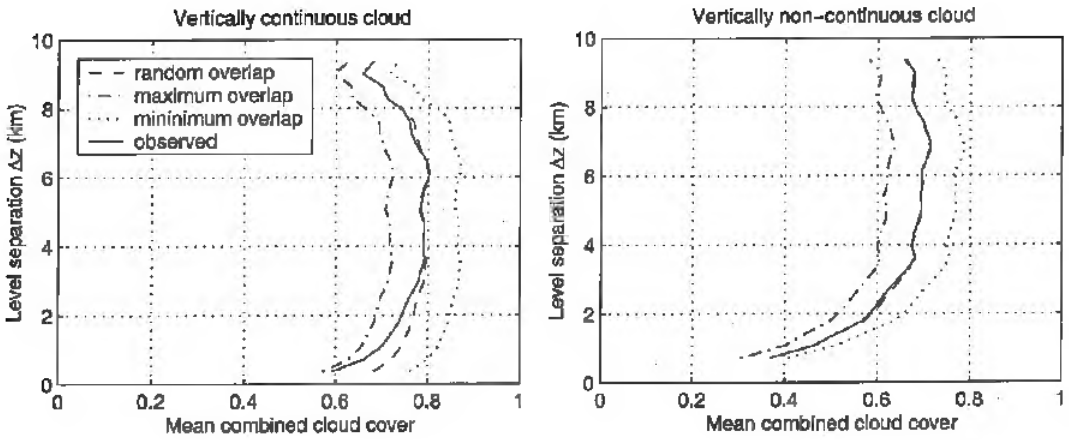

FIG. 3: The mean observed combined cloud cover of pairs of levels as a function of level separation (solid line), together with the values calculated using three different overlap assumptions. The vertical resolution was 360 m and the temporal resolution was 1 hour. Only events where the cloud cover at both levels was greater than zero and less than one were used. The left panel was compiled from events for which every intermediate level contained some cloud and the right panel corresponds to cases for which at least one of the intermediate levels was entirely cloud-free.

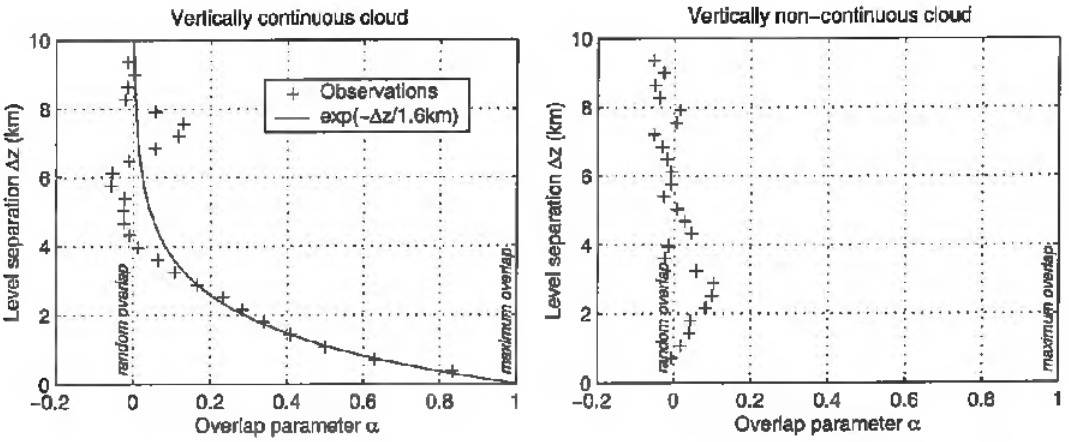

FIG. 4: The overlap parameter α versus level separation for vertically continuous and non-continuous cloud, using boxes 360 m in height and 1 hour in duration. A value of unity indicates maximum overlap and a value of zero indicates random overlap.

Vertical resolution	Temporal resolution		
	20 mins	1 hour	3 hours
360 m	1.40 km	1.60 km	2.04 km
720 m	1.68 km	1.90 km	2.30 km
1080 m	2.04 km	2.15 km	2.48 km
1440 m	2.54 km	2.56 km	2.93 km

TABLE 1: Values of the e-folding distance Δz_0 for different vertical and temporal resolutions.

some possible statistical noise is apparent in α for level separations of more than 7 km. Nonetheless, it is remarkable that as little as a few days of data are sufficient to exhibit essentially the same overlap behaviour as shown in Fig. 4, indicating that this 71 day dataset is easily long enough to derive robust values of Δz_0.

It can be seen from Table 1 that a decrease in either temporal or vertical resolution results in an increase in Δz_0 and thus an increase in the degree of overlap for a given level separation. The change with temporal resolution can be explained by considering an isolated cloud; as the box becomes larger the cloud will occupy a decreasing fraction of the box and the apparent degree of overlap must increase. Indeed, the degree of overlap can never decrease with decreasing temporal resolution. A reduction in vertical resolution can, in individual cases, result in either an increase or a decrease in the degree of overlap, but it simply turns out that the former is more common, particularly for adjacent levels. It is found that Δz_0 does not have a significant dependence on whether the pairs of levels are taken from the upper or lower troposphere. One interesting finding is that with a temporal resolution of 3 hours and a level separation of between 6 and 8 km, α falls to −0.1, indicating a tendency for a lower degree of overlap than even that predicted by the random overlap assumption. The reason for this is that in Southern England during winter, fronts are almost entirely responsible for clouds more than 5 km thick, and these have a char-

acteristic 'slanted' signature in radar time-height sections that can only really be detected in sections of 3 hours or longer (Fig. 2 is a striking example).

4. Conclusions

A simple method for using long-term radar observations to characterise cloud overlap has been developed that expresses mean overlap in a way that could be implemented in GCMs. It has been found that the mean overlap of vertically continuous clouds is distinctly more random than models usually assume, and this will probably have a significant effect on the predictions made with such models. Before applying the findings of this study to global models it would be advisable to use the technique to derive overlap statistics from cloud radars in other locations, and in all seasons, since the overlap characteristics of convective clouds may be appreciably different from those of frontal clouds. A number of 35-GHz cloud radars have recently been deployed at various locations around the globe as part of the Atmospheric Radiation Measurement program (Moran et al. 1998), which would be ideally suited to this task. It would also be a useful application of the proposed spaceborne 94-GHz radar on board 'CloudSat', which is scheduled for launch in spring 2003 as part of the NASA Earth System Science Pathfinder program.

Acknowledgements. We are grateful to the Radio Communications Research Unit at the Rutherford Appleton Laboratory for the use of the Galileo radar, which was developed for the European Space Agency by Officine Galileo, the Rutherford Appleton Laboratory and the University of Reading, under ESTEC Contract No. 10568/NL/NB. Our thanks go to Christian Jakob for providing the ECMWF model data and for some useful discussions. This research received funding from NERC grant GR3/8765.

REFERENCES

Barker, H. W., Stephens, G. L., and Fu, Q., 1999: The sensitivity of domain-averaged solar fluxes to assumptions about cloud geometry. *Quart. J. Roy. Meteor. Soc.*, **125**, 2127–2152.

Brown, P. R. A., Illingworth, A. J., Heymsfield, A. J., McFarquhar, G. M., Browning, K. A., and Gosset, M., 1995: The role of spaceborne millimeter-wave radar in the global monitoring of ice-cloud. *J. Appl. Meteor.*, **34**, 2346–2366.

Charnock, T., Rose, F., Alberta, T., Smith, G. L., Rutan, D., Manalo-Smith, N., Minnis, P., and Wielicki, B., 1994: Cloud profiling radar requirements: Perspective from retrievals of the surface and atmospheric radiation budget and studies if atmospheric energetics. In *Utility and feasibility of a cloud profiling radar.* Report of the GEWEX Tropical Workshop, 2–29 July 1993, Pasadena, California, IGPO 10, pp. B10–B21.

Geleyn, J. F., and Hollingsworth, A., 1979: An economical analytical method for the computation of the interaction between scattering and line absorption of radiation. *Contrib. Atmos. Phys.*, **52**, 1–16.

Hogan, R. J., and Illingworth, A. J., 1999: Analysis of radar and lidar returns from clouds: Implications for the proposed Earth Radiation Mission. *CLARE'98 Final Workshop, 13–14 September 1999*, ESA/ESTEC, Noordwijk, The Netherlands.

Hogan, R. J., Jakob, C., and Illingworth, A. J., 2001: Comparison of ECMWF cloud fraction with radar derived values. *J. Appl. Meteor.*, in press.

International Panel on Climate Change (IPCC), 1995: *IPCC Second Assessment Report—Climate Change 1995*. UNEP/WMO.

Jakob, C., and Klein, S. A., 1999: The role of vertically varying cloud fraction in the parametrization of microphysical processes in the ECMWF model. *Quart. J. Roy. Meteor. Soc.*, **125**, 941–965.

Liang, X.-Z., and Wang, W.-C., 1997: Cloud overlap effects on general circulation model simulations. *J. Geophys. Res.*, **102**, 11039–11047.

Liou, K.-N., and Zheng, Q., 1984: A numerical experiment on the interactions of radiation, clouds and dynamical processes in a general circulation model. *J. Atmos. Sci.*, **41**, 1513–1535.

Mace, G. G., Jakob, C., and Moran, K. P., 1998: Validation of hydrometeor occurrence predicted by the ECMWF model using millimeter wave radar data. *Geophys. Res. Lett.*, **25**, 1645–1648.

Moran, K. P., Martner, B. E., Post, M. J., Welsh, D. C., and Widener, K. B., 1998: An unattended cloud-profiling radar for use in climate research. *Bull. Am. Meteorol. Soc.*, **79**, 443–455.

Morcrette, J. J., and Fouquart, Y., 1986: The overlapping of cloud layers in shortwave radiation parameterization. *J. Atmos. Sci.*, **43**, 321–328.

Morcrette, J. J., and Jakob, C., 2000: The response of the ECMWF model to changes in cloud overlap assumption. *Mon. Weath. Rev.*, in press.

Randall, D. A., Harshvardhan, Dazlich, D. A., and Corsetti, T. G., 1989: Interactions among radiation, convection and large-scale dynamics in a general-circulation model. *J. Atmos. Sci.*, **64**, 1943–1970.

Slingo, A., and Slingo, J. M., 1988: The response of a general circulation model to cloud long-wave radiative forcing. I: Introduction and initial experiments. *Quart. J. Roy. Meteor. Soc.*, **114**, 1027–1062.

Stubenrauch, C. J., DelGenio, A. D., and Rossow, W. B., 1997: Implementation of subgrid cloud vertical structure inside a GCM and its effect on the radiation budget. *J. Climate*, **10**, 273–287.

Tian, L., and Curry, J. A., 1989: Cloud overlap statistics. *J. Geophys. Res.*, **94**, 9925–9935.

CURRENT JCMM INTERNAL REPORTS

This series of JCMM Internal Reports, initiated in 1993, contains unpublished reports and also versions of articles submitted for publication. The complete set of Internal Reports is available from the National Meteorological Library on loan, if required.

1. **Research strategy and programme**
   K A Browning et al
   January 1993

2. **The GEWEX Cloud System Study (GCSS)**
   GEWEX Cloud System Science Team
   January 1993

3. **Evolution of a mesoscale upper tropospheric vorticity maximum and comma cloud from a cloud-free two dimensional potential vorticity anomaly**
   K A Browning
   January 1993

4. **The global energy and water cycle**
   K A Browning
   July 1993

5. **Structure of a midlatitude cyclone before occlusion**
   K A Browning and N Roberts
   July 1993

6. **Developments in systems and tools for weather forecasting**
   K A Browning and G Szejwach
   July 1993

7. **Diagnostic study of a narrow cold frontal rainband and severe winds associated with a stratospheric intrusion**
   K A Browning and R Reynolds
   August 1993

8. **Survey of perceived priority issues in the parametrizations of cloud-related processes in GCMs**
   K A Browning
   September 1993

9. **The effect of rain on longwave radiation**
   I Dharssi
   September 1993

10. **Cloud microphysical processes - a description of the parametrization used in the large eddy model**
    H Swann
    October 1993

11. **An appreciation of the meteorological research of Ernst Kleinschmidt**
    A J Thorpe
    May 1992

12. **Potential vorticity of flow along the Alps**
    A J Thorpe, H Volkert and Dietrich Heimann
    August 1992

13. **The representation of fronts**
    A J Thorpe
    January 1993

14. **A parametrization scheme for symmetric instability: test for an idealised flow**
C S Chan and A J Thorpe
February 1993

15. **The Fronts 92 Experiment: a Quicklook Atlas**
Edited by T D Hewson
November 1993

16. **Frontal wave stability during moist deformation frontogenesis**
Part 1: Linear wave dynamics
C H Bishop and A J Thorpe
May 1993

17. **Frontal wave stability during moist deformation frontogenesis**
Part 2. The suppression of non-linear wave development
C H Bishop and A J Thorpe
May 1993

18. **Gravity waves in sheared ducts**
S Monserrat and A J Thorpe
October 1993

19. **Potential vorticity and the electrostatics analogy: quasi-geostrophic theory**
C Bishop and A J Thorpe
November 1993

20. **Recent advances in the measurement of precipitation by radar**
A J Illingworth
April 1993

21. **Micro-physique et givrage: cloud microphysics and aircraft icing**
A J Illingworth
May 1993

22. **Differential phase measurements of precipitation**
M Blackman and A J Illingworth
May 1993

23. **Estimation of effective radius of cloud particles from the radar reflectivity**
N I Fox and A J Illingworth
May 1993

24. **A simple method of Dopplerising a pulsed magnetron radar**
A Hua, A J Illingworth and J Eastment
November 1993

25. **Radiation and polar lows**
George C Craig
February 1994

26. **Collected preprints submitted to the International Symposium on the Life Cycles of Extratropical Cyclones; Bergen, Norway, 27 June - 1 July 1994**
April 1994

27. **Convective frontogenesis**
Douglas J Parker and Alan J Thorpe
April 1994

28. **Improved measurement of the ice water content in cirrus using a total water evaporator**
Philip R A Brown and Peter N Francis
April 1994

29. **Mesoscale effects of a dry intrusion within a vigorous cyclone**
K A Browning and B W Golding
April 1994

30. **GEWEX Cloud System Study, Science Plan**
May 1994

31. **Parametrization of momentum transport by convectively generated gravity waves**
R Kershaw
May 1994

32. **Mesoscale Modelling Newsletter No 5**
May 1994

33. **Observations of the mesoscale sub-structure in the cold air of a developing frontal cyclone**
K A Browning, S A Clough, C S A Davitt, N M Roberts and T D Hewson
May 1994

34. **Longwave radiative forcing of a simulated tropical squall line**
Imtiaz Dharssi
July 1994

35. **On the nature of the convective circulation at a kata-cold front**
K A Browning
September 1994

36. **Collective preprints of papers submitted to the COST-75 International Seminar on Advanced Weather Radar Systems, Brussels, 20-23 September 1994**
November 1994

37. **Use of satellite imagery to diagnose events leading to frontal thunderstorms: Parts I and II of a case study**
K A Browning and N M Roberts
November 1994

38. **The role of spaceborne millimetre-wave radar in the global monitoring of ice cloud**
P R A Brown, A J Illingworth, A J Heymsfield, G M McFarquhar, K A Browning and M Gosset
December 1994

39. **Potential vorticity inversion**
Michal Ziemianski
October 1994

40. **Theory of mature tropical cyclones; a comparison between Kleinschmidt (1951) and Emanuel (1986)**
Suzanne L Gray
December 1994

41. **Dispersion and removal of pollutants during the passage of an atmospheric frontal system**
N R Gimson
December 1994

42. **The role of snow sublimation in frontogenesis**
D J Parker and A J Thorpe
December 1994

43. **Potential vorticity and the electrostatics Analogy: Ertel-Rossby formulation**
A J Thorpe and C H Bishop
December 1994

44. **Mesoscale aspect of extratropical cyclones: an observational perspective**
K A Browning
January 1995

45. **A polar low outbreak: evolution and mesoscale structures**
T D Hewson, G C Craig and C Claud
February 1995

46. **Generation of near-surface gusts of deep convection**
K Nakamura and R Kershaw
April 1995

47. **Attribution concepts applied to the Omega Equation**
S A Clough, C S A Davitt and A J Thorpe
June 1995

48. **Parametrization of mixed-phase cloud and precipitation**
Susan P Ballard and M Gerard Hutchinson
June 1995

49. **Short-range forecasting of stratocumulus: initialization prediction**
Susan P Ballard, Simon D Jackson and B Macpherson
June 1995

50. **Contributions of the JCMM/Dept of Meteorology Radar Group to the 27th AMS Radar Meteorology Conference, Vail October 1995**
June 1995

51. **Cold pools in shear**
Douglas J Parker
September 1995

52. **High-resolution analysis of frontal fracture**
K A Browning, S P Ballard and C S A Davitt
September 1995

53. **The albedo of broken cloud fields: calculations using a modified two stream radiation code**
Imtiaz Dharssi and Roy Kershaw
October 1995

54. **Parametrization of momentum transport by convection. I: theory and cloud modelling results**
R Kershaw and D Gregory
November 1995

55. **Variation of frontal structure along a cold front**
K A Browning and N M Roberts
November 1995

56. **Secondary frontal waves**
Douglas Parker
December 1995

57. **Objective fronts**
T D Hewson
March 1996

58. **Mesoscale analysis of the activation of a cold front during cyclogenesis**
K A Browning, N M Roberts and A J Illingworth
June 1996

59. **Investigation of different representations of rain in a 1-d evaporation model**
H Swann
May 1996

60. **Parametrization of diabatic processes in the inversion of the omega-equation**
M Athanassiadou and A J Thorpe
June 1996

61. **The role of the environmental flow in the development of secondary frontal cyclones**
I A Renfrew, A J Thorpe and A Joly
June 1996

62. **Consequences of the geostrophic momentum approximation on barotropic instability**
S Malardel, A J Thorpe and A Joly
June 1996

63. **Contributions to the AMS/RMS Conference on Mesoscale Processes**
Reading, 9-13 September 1996

64. **Vorticity and potential vorticity in stratified flows interacting with an isolated obstacle**
Jorge A Gutiérrez and A J Thorpe
September 1996

65. **Triple point development: two case studies**
Douglas Parker
September 1996

66. **Radar observations of wind-shear splitting within evolving atmospheric Kelvin-Helmholtz billows**
D Chapman and K A Browning
April 1997

67. **Cold frontal structure derived from radar wind profilers**
K A Browning, D Jerrett, J Nash, T Oakley and N M Roberts
May 1997

68. **The dry intrusion and its effect on the frontal, cloud and precipitation structure of extratropical cyclones**
K A Browning - Text of invited special lecture at the Spring Conference
of the Meteorological Society of Japan, University of Tsukuba, 22 May 1997

69. **Met. Office Unified Model data, diagnostics, graphics programs, and other observational data available from the JCMM through the aegis of the Universities Weather Research Network (UWERN).** (Plus supplement)
Peter Panagi and Ed Dicks
June 1997

70. **Contributions of the JCMM/Dept of Meteorology Radar Group to the 28th AMS Radar Meteorology Conference.** Austin, Texas
September 1997

71. **Sensitivity of short-range weather forecasts to local potential vorticity modifications**
Meral Demirtas and Alan Thorpe
July 1997

72. **Objective identification of frontal wave cyclones**
T D Hewson
August 1997

73. **Attribution and its application to mesoscale structure associated with tropopause folds**
A J Thorpe
September 1997

74. **The role of the environmental flow in the development of secondary frontal cyclones**
Ian A Renfrew, Alan J Thorpe and Craig H Bishop
September 1997

75. **Potential vorticity: a short history of its definitions and uses**
Alan J Thorpe and Hans Volkert
September 1997

76. **Superposing semi-geostrophic potential vorticity anomalies**
H R Birkett and A J Thorpe
September 1997

77. **Short period forecasting of catchment-scale precipitation.**
Part 1: the role of Numerical Weather Prediction
M A Pedder, M Haile and A J Thorpe
September 1997

78. **Verification of the tracking technique used in an experimental cloud motion wind inferring system**
Z Wang, K A Browning and G A Kelly
October 1997

79. **A preliminary study of Fourier series analysis for cloud tracking with GOES high temporal resolution images**
Z Wang
October 1997

80. **Analysis of an ex-tropical cyclone after reintensifying as a warm-core extratropical cyclone**
K A Browning, G Vaughan and P Panagi
November 1997

81. **A JCMM overview of FASTEX IOPs**
S A Clough, H W Lean, N M Roberts, H Birkett, J-P Chaboureau, R Dixon, M Griffiths, T D Hewson and A Montani
January 1998

82. **Programs for PV inversion and modification**
Meral Demirtas
December 1997

83. **Release of potential shearing instability in warm frontal zones**
D Chapman and K A Browning
February 1998

84. **The European Cloud-Resolving Modelling Programme (EUCREM)**
Summary Report from the coordinator
P W White
April 1998

85. **A frontal wave database**
T D Hewson
April 1998

86. **Layering observed in dropsoundings from IOP 1 of Fronts 92**
S A Clough
May 1998

87. **Use of wind-shear displays for Doppler radar data**
D Chapman and K A Browning
May 1998

88. **Radar estimates of rainfall rates at the ground in bright band and non-bright band events**
T J Smyth and A J Illingworth
June 1998

89. **Correction for attenuation of radar reflectivity using polarisation data**
T J Smyth and A J Illingworth
June 1998

90. **The effects of convection on chemical reactions and precipitation scavenging**
Neil R Gimson
July 1998

91. **How to use the display program DISP**
Nigel Roberts
August 1998

92. **Conceptual models of cyclogenesis**
Adrian T Semple
August 1998

93. **Observations of oblate hail using dual polarisation radar and implications for hail detection schemes**
T J Smyth, T M Blackman and A J Illingworth
September 1998

94. **The semigeostrophic diagnosis of vertical motion. Part I: Formulation and co-ordinate transformations**
Mike A Pedder and Alan J Thorpe
September 1998

95. **The semigeostrophic diagnosis of vertical motion. Part II: Results for an idealised baroclinic wave life cycle**
Alan J Thorpe and Mike A Pedder
September 1998

96. **Convective destabilisation by a tropopause fold diagnosed using potential vorticity inversion**
Morwenna Griffiths, Alan Thorpe and Keith Browning
October 1998

97. **Forecast skill of the ECMWF model using targeted observations during FASTEX**
A Montani, A J Thorpe, R Buizza and P Unden
October 1998

98. **Observations and model simulations of the FASTEX IOP 16 frontal wave - effects of sublimation**
Sid A Clough, Humphrey W Lean, Nigel M Roberts and Richard M Forbes
December 1998

99. **The application of conceptual models in NWP**
Adrian T Semple
January 1999

100. **Mesoscale analysis of arc rainbands in a dry slot**
K A Browning and N M Roberts
January 1999

101. **Interaction of mesoscale tropopause depressions with a warm-core cyclone: observational and model analyses, and sensitivity to analysis errors**
K A Browning, A J Thorpe, A Montani, D Parsons, M Griffiths, P Panagi and E M Dicks
February 1999

102. **The use of water vapour imagery and PV inversion to adjust initial conditions in NWP**
Sean J Swarbrick
February 1999
This report is no longer available; see Internal Report No.108

103. **Summary notes for a lecture course on Waves in the Atmosphere and Ocean**
A A White
March 1999

104. **Results of a questionnaire on the operational value of conceptual models (CMs) of fronts and cyclones**
N M Roberts & M V Young
July 1999

105. **Contributions to the Poster Session at the 1998 UWERN Annual Science Meeting**
assembled by A A White
August 1999

106. **The objective analysis of dropsonde data from FASTEX**
Richard Forbes, Sid Clough, Mark Dixon, Andy Macallan & Nigel Roberts
January 2000

107. *NWP Technical Report No.302*
Implications for Mesoscale Modelling from a Study of the FASTEX IOP 16 Mid-latitude Cyclone
Richard M Forbes, Humphrey W Lean, Nigel M Roberts and Peter A Clark
March 2000

108. *NWP Technical Report No.291*
The use of water vapour imagery and PV inversion to adjust initial conditions in NWP
Final Project Report
Sean J Swarbrick
September 1999

109. *NWP Technical Report No.294*
A guide to aspects of water vapour imagery interpretation: the significance of dry regions
Nigel M Roberts
January 2000

110. *NWP Technical Report No.300*
The relationship between water vapour imagery and thunderstorms
Nigel M Roberts
February 2000

111. *NWP Technical Report No.293*
Holomorphic structures in hydrodynamical models of nearly geostrophic flow
V N Roubtsov and I Roulstone
January 2000

112. *NWP Technical Report No.301*
Multi-sensor synthesis of the mesoscale structure of a cold-air comma cloud system
K A Browning, P Panagi and E M Dicks
March 2000

113. *NWP Technical Report No.307*
Observations of stratospheric air entering the circulation of a polar low
K A Browning and E M Dicks
May 2000

114. *NWP Technical Report No.309*
Wind profiler – Unified Model comparison statistics
Peter Panagi & Ed Dicks
March 2000

115. *NWP Technical Report No.310*
Towards a similarity theory of moist convective updrafts
Olaf Stiller and George C Craig
May 2000

116. *NWP Technical Report No.312*
The mystery of striated cloud heads in satellite imagery
R S Dixon, K A Browning and G J Shutts
April 2000

117. *NWP Technical Report No.313*
MDIAG: a Fortran 90 program to compute diagnostics on pressure levels from Unified Model data on model levels
Peter Panagi
June 2000

118. *NWP Scientific Paper No.56*
Rearrangements of functions with applications to meteorology and ideal fluid flow
R J Douglas
June 2000

119. *NWP Technical Report No.320*
Tests of New Dynamics Model on the FASTEX IOP16 case
Humphrey Lean
September 2000

120. *NWP Scientific Paper 57*
A classification of FASTEX cyclones using a height-attributable QG vertical motion diagnostic
A C L Deveson, K A Browning, T D Hewson
September 2000

121. *NWP Scientific Paper 59*
Measurements of dissipation rate in frontal zones
D.Chapman, K A Browning
August 2000

122. *NWP Technical Report 331*
Not Issued yet

123. *NWP Technical Report 337*
A Case Study of High Resolution Fog Forecasts with the New Dynamics
P. Clark
November 2000

124. *NWP Technical Report 338*
Comparison of ECMWF Winter-Season Cloud Fraction with Radar Derived Values
Robin J. Hogan, Christian Jakob, Anthony J. Illingworth
January 2001

125. *NWP Technical Report 339*
Deriving Cloud overlap statistics from radar
Robin J. Hogan, Anthony J. Illingworth
January 2001

Met Office Joint Centre for Mesoscale Meteorology Department of Meteorology
University of Reading PO Box 243 Reading RG6 6BB United Kingdom
Tel: +44 (0)118 931 8425 Fax: +44 (0)118 931 8791
www.metoffice.com